



HAL
open science

Claudin 11 deficiency in mice results in loss of the Sertoli cell epithelial phenotype in the testis.

Séverine Mazaud-Guittot, Emmanuelle Meugnier, Sandra Pesenti, Xin Wu, Hubert Vidal, Alexander Gow, Brigitte Le Magueresse-Battistoni

► **To cite this version:**

Séverine Mazaud-Guittot, Emmanuelle Meugnier, Sandra Pesenti, Xin Wu, Hubert Vidal, et al..
Claudin 11 deficiency in mice results in loss of the Sertoli cell epithelial phenotype in the testis..
Biology of Reproduction, 2010, 82 (1), pp.202-13. 10.1095/biolreprod.109.078907 . inserm-00816455

HAL Id: inserm-00816455

<https://inserm.hal.science/inserm-00816455>

Submitted on 22 Apr 2013

HAL is a multi-disciplinary open access archive for the deposit and dissemination of scientific research documents, whether they are published or not. The documents may come from teaching and research institutions in France or abroad, or from public or private research centers.

L'archive ouverte pluridisciplinaire **HAL**, est destinée au dépôt et à la diffusion de documents scientifiques de niveau recherche, publiés ou non, émanant des établissements d'enseignement et de recherche français ou étrangers, des laboratoires publics ou privés.

Claudin 11 Deficiency in Mice Results in Loss of the Sertoli Cell Epithelial Phenotype in the Testis¹

S. Mazaud-Guittot,^{3,4,5,6,7,8} E. Meugnier,^{4,5,6,7,8} S. Pesenti,^{4,5,6,7,8} X. Wu,⁹ H. Vidal,^{4,5,6,7,8} A. Gow,^{9,10,11}
and B. Le Magueresse-Battistoni^{2,4,5,6,7,8}

INSERM, U870,⁴ Oullins, France

INRA, UMR1235,⁵ Oullins, France

INSA-Lyon,⁶ RMND, Villeurbanne, France

Université Lyon 1,⁷ Lyon, France

Hospices Civils de Lyon,⁸ Lyon, France

Center for Molecular Medicine and Genetics,⁹ Karman and Ann Adams Department of Pediatrics,¹⁰ and Department of Neurology,¹¹ Wayne State University, Detroit, Michigan

ABSTRACT

Tissue integrity relies on barriers formed between epithelial cells. In the testis, the barrier is formed at the initiation of puberty by a tight junction complex between adjacent Sertoli cells, thereby defining an adluminal compartment where meiosis and spermiogenesis occur. Claudin 11 is an obligatory protein for tight junction formation and barrier integrity in the testis. It is expressed by Sertoli cells, and spermatogenesis does not proceed beyond meiosis in its absence, resulting in male sterility. Sertoli cell maturation—arrest of proliferation and expression of proteins to support germ cell development—parallels tight junction assembly; however, the pathophysiology underlying the loss of tight junctions in the mature testis remains largely undefined. Here, using immunohistochemistry and microarrays we demonstrate that adult *Cldn11*^{-/-} mouse Sertoli cells can proliferate while maintaining expression of mature markers. Sertoli cells detach from the basement membrane, acquire a fibroblast cell shape, are eliminated through the lumen together with apoptotic germ cells, and are found in epididymis. These changes are associated with tight junction regulation as well as actin-related and cell cycle gene expression. Thus, *Cldn11*^{-/-} Sertoli cells exhibit a unique phenotype whereby loss of tight junction integrity results in loss of the epithelial phenotype.

blood-testis barrier, gene regulation, Sertoli cells, spermatogenesis, testis

¹Supported by the Institut National de la Santé et de la Recherche Médicale (INSERM), Institut National et de la Recherche Agronomique (INRA), University Lyon I, and partly from grants to B.L.M.B. by ANR (ANR-06-PNRA-006) and AFSSET (EST-2006/1/33), and grants by the National Institute on Deafness and Other Communication Disorders, National Institutes of Health (DC006262) to A.G.

²Correspondence: B. Le Magueresse-Battistoni, INSERM U870, INRA UMR 1235, 165 Chemin du Grand Revoyet, BP 12, 69921 Oullins cedex France. FAX: 33 4 26235916; e-mail: Brigitte.lemagueresse@inserm.fr

³Correspondence and current address: S. Mazaud-Guittot, INSERM U625, Rennes, France, and University Rennes I, Campus de Beaulieu, IFR-140, GERHM, Rennes, F-35042, France. FAX: 33 2 2325055; e-mail: severine.mazaud@univ-rennes1.fr

Received: 15 May 2009.

First decision: 16 June 2009.

Accepted: 31 August 2009.

© 2010 by the Society for the Study of Reproduction, Inc.

This is an Open Access article, freely available through *Biology of Reproduction's* Authors' Choice option.

eISSN: 1529-7268 <http://www.biolreprod.org>

ISSN: 0006-3363

INTRODUCTION

The integrity of epithelial cell layers is maintained by intercellular junctional complexes composed of adhesive (adherens junction, desmosomes) and occluding (tight) junctions, and gap junctions promote intercellular communication. The transmembrane proteins constituting these junctions are linked to components of the actin and intermediate filament cytoskeletons, and a growing number of cytoplasmic scaffolding molecules associated with these junctions are involved in regulating such diverse processes as transcription, cell proliferation, cell polarity, and the assembly of regulated diffusion barriers. Typically, tight junctions (TJs) define the boundary between the apical and basolateral domains of epithelial cell membranes and function as the primary barrier to diffusion of macromolecules, ions, and small noncharged solutes through the paracellular pathway [1, 2].

Most blood-tissue barriers, such as the blood-brain and blood-retinal barriers, are generated by endothelial cell TJs in specialized microvessels. By contrast, the blood-testis barrier (BTB) is generated and maintained by Sertoli cells in the seminiferous epithelium and is physically remote from microvessels of the interstitium. The BTB is also unique because it is cyclically restructured during spermatogenesis when preleptotene spermatocytes migrate into the adluminal compartment and enter meiosis. Thus, the BTB divides the seminiferous epithelium into two compartments: the basal compartment, which forms the niche for spermatogonia proliferation and renewal, and the adluminal compartment, where meiosis and spermiogenesis occur.

Both the structural integrity of the seminiferous epithelium and the BTB are maintained by the highly specialized actin filament network of the Sertoli cell cytoskeleton, known as the ectoplasmic specialization (ES). Ectoplasmic specializations are complex cytoskeletal structures occurring in submembranous regions adjacent to TJs (BTB) and the apical adhesion sites of spermatogenic cells [3–6]. They consist of bundles of actin filaments sandwiched between the plasma membrane and cisternae of the endoplasmic reticulum [3–7]. Because they are closely associated with junctional sites, ESs are thought to play a major role in maintaining and regulating intercellular junction assembly [3, 8–14].

The molecular composition of the BTB has been the subject of numerous studies reviewed in Lui and Cheng [15], and Sertoli cell TJs are composed, at least, of the transmembrane proteins claudin 11, claudin 3, occludin, junction-associated molecule (JAM-A; official symbol F11R), and the coxsackie

TABLE 1. List of primer sequences used for RT-qPCR.

Gene symbol	Accession no.	5'→3' Forward primer	5'→3' Reverse primer	Amplicon size
<i>Mtdh</i>	NM_026002	CACACAGGACACAGAAGACC	CAGAGATAGCAGGAGGAAGAG	179
<i>Fyn</i>	NM_008054	CAGCAAGACAAGGTGCGAAG	TGTGGGCAGGGCATCCTATAGC	205
<i>Espn</i>	NM_019585	AAGAGGAGCAGCGGAGGAAG	TCCTCTTTTCGCTTCTGCTC	121
<i>Exoc4</i>	NM_009148	AGACATCAGTGCCATGGAAG	CGTGACATGGTGATGTTTG	207
<i>Csda</i>	NM_011733	CACCAAAGTCCCTGGCACTG	CCTTCAACTACATCAAACCTC	180
<i>Tjp1</i>	NM_009386	ACGCATCACAGCCTGGTTG	TGGCTCCTTCTGTACACC	122
<i>Lasp1</i>	NM_010688	AGCAGCCCTGTCTCCATAC	TCATCGATCTGCTGCACATTG	144
<i>Rpl19</i>	NM_009078	CTGAAGTCAAAGGGAATGTG	GGACAGAGTCTTGATGATCTC	195

virus and adenovirus receptor (CAR; official symbol CXADR) [15, 16]. The phenotypes of mice deficient in various components of these TJs vary from normal (no apparent phenotype), as revealed in *Fllr*^{-/-} mice [17], to slowly degenerative, as for *Ocln*^{-/-} mice [18], to sterility in *Cldn11*^{-/-} mice [19]. *Cldn11*^{-/-} mice exhibit neurologic, auditory, and reproductive deficits, including slowed central nervous system nerve conduction, conspicuous hind limb weakness, profound sensorineural deafness, and male sterility [19–21].

In the testis of *Cldn11*^{-/-} mice, spermatogenesis does not proceed beyond the spermatocyte stage, and cell clusters are observed in the seminiferous lumen. To understand the relationship between claudin 11 loss and seminiferous tubule disorganization, we have determined the etiology of this phenotype, in particular during the period when the BTB forms. Our comprehensive survey reveals that the absence of a mature BTB in Sertoli cells lacking claudin 11 [19] is linked to a spermatogenesis defect in neighboring germ cells. Furthermore, Sertoli cells lose polarity, detach from the basement membrane, undergo an epithelial-to-fibroblastic cell shape transformation, and proliferate while maintaining expression of differentiation markers. These changes are associated with TJ regulation as well as actin-related and cell cycle gene expression.

MATERIALS AND METHODS

Animal Handling, Tissue Collection, and Processing

Claudin 11-null mice [19] were maintained on a mixed genetic background comprising 129SvEv and C57BL6/J strains and have been brother-sister mated for more than 10 generations. The testicular phenotype has been stable in this colony for 10 yr. Males were injected intraperitoneally with 50 mg/kg bromodeoxyuridine (BrdU) dissolved in saline 3 h before killing. Testes and epididymides collected at Postnatal Day 7 (P7), P10, P13, P15, P20, P28, P60, P90, and P180 were either frozen on dry ice and stored at -80°C until processing for RNA analysis or were processed for morphological studies. For histological and immunohistochemical analyses, tissues were fixed either in Bouin fixative or in 4% paraformaldehyde-PBS (pH 7.2) for at least 24 h, dehydrated in a graded series of ethanol, and paraffin embedded using standard protocols. Five-micrometer-thick sections were stained with the periodic acid-Schiff-hematoxylin technique (PAS). All experiments on claudin 11 mice were performed at Wayne State University and were conducted within the guidelines and protocols approved by the Institutional Animal Care and Use committee.

Immunohistochemistry

Paraffin-embedded tissues were deparaffinized in xylene and rehydrated in graded ethanol solutions, and endogenous peroxidase activity was blocked with 0.3% hydrogen peroxide in methanol for 30 min. For all but claudin 11 immunodetection, sections were boiled for 5 min in 0.1 M citrate buffer (pH 6.0) for antigen retrieval, blocked with 10% horse serum (in PBS with 8% bovine serum albumin) for at least 20 min, and finally incubated overnight at 4°C with primary antibody diluted in blocking solution (Dako Corp., Trappes, France). For claudin 11 immunodetection, sections underwent the same process except that the antigen retrieval step was omitted. Primary antibodies were directed against claudin 11 (diluted 1:100; Santa Cruz Biotechnologies Inc., Santa Cruz, CA), DDX4 (diluted 1:750; kindly provided by Dr. T. Noce,

Mitsubishi Kagaku Institute of Life Sciences, Tokyo, Japan), Clgn (TRA-369 antibody; diluted 1:1000; kindly provided by Dr. H. Tanaka, Osaka University, Osaka, Japan), Gata4 (diluted 1:100; Santa Cruz Biotechnologies), phosphorylated serine 10 (ser10) of histone H3 (diluted 1:500; Upstate Biotechnology/Euromedex, Mundolsheim, France), BrdU (diluted 1:100; Roche), and vimentin (LN-6 clone; diluted 1:100; DakoCytomation, Trappes, France).

After washing in PBS, and depending on the primary antibody used, sections were incubated for 2 h with either horseradish peroxidase-conjugated anti-rabbit antibody (Envision+ system-HRP; Dako), biotinylated anti-goat antibody (1:500 dilution; Vector Laboratories Canada, Burlington, ON, Canada), or anti-rat antibody (1:200 dilution; Vector Laboratories), and finally for 30 min with a peroxidase-conjugated streptavidin-horseradish complex (LSAB+ Kit; Dako). The reaction product was developed using 3,3'-diaminobenzidine tetrahydrochloride (DAB; Sigma-Aldrich). Sections were counterstained with hematoxylin and mounted with Eukitt (Sigma-Aldrich). For negative controls, primary antibody was omitted. Slides were analyzed with Zeiss Akioskop II and Axiophot microscopes (Carl Zeiss, New York, NY) connected to a digital camera (Spot RT Slider; Diagnostic Instruments, Sterling Heights, MI).

For double immunolabeling, paraffin sections were prepared as above and incubated overnight with anti-Gata4 antibody (diluted 1:100), followed by sequential incubations with anti-goat immunoglobulin (Ig)-Alexa Fluor 546 secondary antibody (1:1000; Invitrogen) for 2 h at room temperature, anti-BrdU antibody (1:100), and anti-mouse Ig-Alexa Fluor 488 secondary antibody (1:1000; Invitrogen). Fluorochrome-labeled sections were mounted in Vectashield containing DAPI for nuclei visualization (Vector Laboratories Canada). Slides were analyzed with a Zeiss Axiophot epifluorescence microscope (Carl Zeiss) connected to a digital camera (Spot RT Slider).

TUNEL Assays

Detection of apoptotic cells was performed on paraffin sections using an in situ cell death detection kit (Roche). After rehydration, sections were boiled for 5 min in 0.1 M citrate buffer (pH 6.0) and were incubated for 1 h at 37°C with the TUNEL reaction mixture containing terminal transferase to label free 3'-hydroxy ends of genomic DNA with fluorescein-labeled deoxy-UTP. After washing, sections were incubated overnight at 4°C with peroxidase converter (Roche). Apoptotic cells were revealed with DAB, and sections were counterstained with hematoxylin. Negative controls with the reaction mixture without the enzyme were applied to serial sections and revealed similarly.

Morphometric Analysis

Apoptotic cells and germ cells in the division phases were quantified in transverse seminiferous tubule sections. Fragmented DNA in nucleus of apoptotic cells was stained with TUNEL, and nuclei of dividing cells were labeled with phosphorylated histone H3. For each animal, at least three nonserial testicular sections equally distributed in a half-testis were used, and in each section, all transverse sectioned tubules were quantified, for a total of at least 100 tubules per animal (with a mean of 330 and 300 tubules per animal). In addition, the number of phosphorylated histone H3-labeled cells was counted in at least 50 tubules per animal. Sertoli cell nuclei were quantified in transverse seminiferous tubule sections stained for GATA4. For each animal, at least three nonserial testicular sections were used, and in each section, all transverse section tubules were quantified, for a total of at least 50 tubules per animal.

Microarray Analysis

Total RNA was prepared from P20 testes by using an RNeasy minikit (Qiagen, Courtaboeuf, France). RNA integrity was determined with the Agilent 2100 Bioanalyzer and RNA 6000 Nano Kit (Agilent Technologies, Massy,

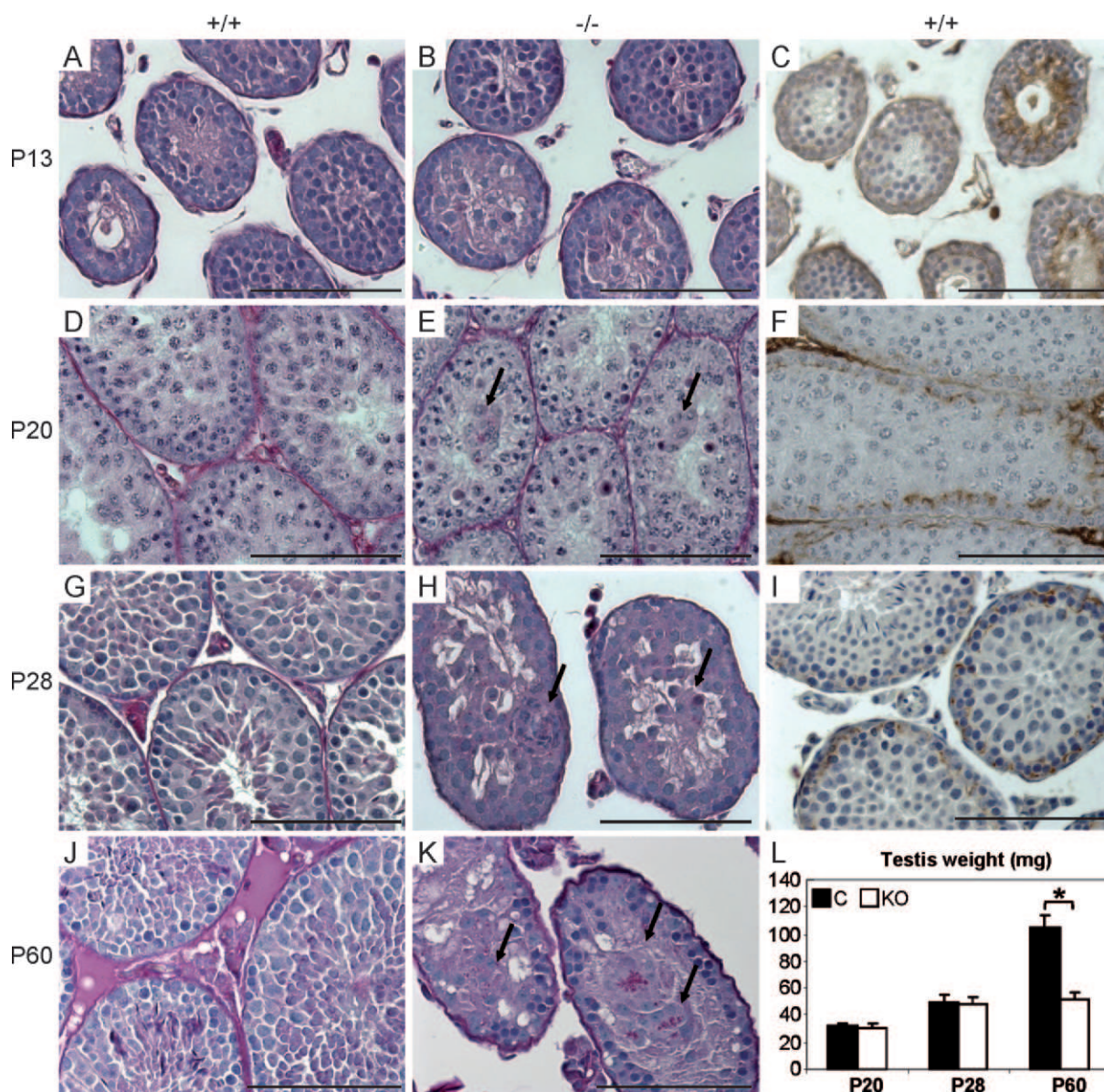


FIG. 1. Chronology of the testis phenotype in *Cldn11*^{-/-} mice. Testicular sections of P13 (A–C), P20 (D–F), P28 (G–I), and P60 (J and K) from control (A, D, G, J, C, F, and I) and *Cldn11*^{-/-} (B, E, H, and K) mice were processed for PAS histological staining (A, B, D, E, G, H, J, and K) and claudin 11 immunohistochemistry (C, F, and I). L) Control (C; black) and *Cldn11*^{-/-} (KO; white) testis weight (n = 3). Arrows point to the round cell clusters. Asterisks indicate statistical significance ($P < 0.001$) by one-way ANOVA followed by Tukey posthoc testing. Bars = 100 μ m.

France). A pool of P20 *Cldn11*^{+/-} testes originating from three different males was used as a common reference and compared to three testes originating from three different *Cldn11*^{-/-} males. One microgram of total RNA was amplified with the Amino Allyl MessageAmp II aRNA kit (Ambion, Austin, TX) according to the manufacturer's instructions. This mRNA amplification procedure is well validated, and it has been demonstrated that it does not distort the relative abundance of individual mRNAs within a RNA population [22].

Fluorescent probes were synthesized by chemical coupling of 5 μ g of aminoallyl aRNA with cyanine 3 (Cy3) or Cy5 dyes (GE Healthcare Biosciences, Orsay, France). After purification with an RNeasy Mini Kit (Qiagen), probes were fragmented with 25 \times RNA Fragmentation Reagents (Agilent Technologies) and hybridized with 2 \times Agilent Hybridization Buffer (Agilent Technologies) to Mouse opArray (Operon Biotechnologies GmbH, Cologne, Germany) in an Agilent oven at 67 $^{\circ}$ C for 16 h, following a dye swap experimental procedure to correct for gene-specific dye bias [23]. Microarrays were washed and scanned with a Genepix 4000B scanner (Molecular Devices).

TIFF images were analyzed using Genepix Pro 6.0 software (Molecular Devices). Signal intensities were log transformed, and normalization was performed by the intensity-dependent Lowess method. To compare results from

the different experiments, data from each slide were normalized in log space to have a mean of zero using Cluster 3.0 software (<http://rana.lbl.gov/EisenSoftware.htm>). Data were analyzed using the Significance Analysis of Microarray (SAM) procedure [24]. Microarray data are available in the Gene Expression Omnibus database under the number GSE15492. Further analysis of GO (www.geneontology.org) and KEGG pathway (www.genome.jp/kegg/pathway.html) enrichments were performed using the WebGestalt analysis toolkit (<http://bioinfo.vanderbilt.edu/webgestalt/>) [25].

Quantitative PCR

Quantitative PCRs were done on RNA from the same three *Cldn11*^{-/-} and three *Cldn11*^{+/-} testes, assessed individually. First-strand cDNAs were synthesized from 1 μ g of total RNA in the presence of 100 units of Superscript II (Invitrogen, Eragny, France) and a mixture of random hexamers and oligo(dT) primers (Promega, Charbonnières, France). Real-time PCR assays were performed in duplicates for each sample with a Rotor-Gene 6000 (Corbett Research, Mortlake, Australia). The PCR primers are listed in Table 1.

Data Analysis

Statistical analyses were performed using the SigmaStat 2.0 software package. For cell counts, a one-way ANOVA followed by the appropriate posthoc test was used to compare differences between groups, as specified in each figure legend. Significance was accepted at a confidence level of $P \leq 0.05$.

RESULTS

Chronology of the *Cldn11*^{-/-} Phenotype

To characterize the beginning of the testicular phenotype in *Cldn11*^{-/-} mice, we first analyzed testis histological sections throughout postnatal testicular development (Fig. 1). During normal testis development, at 2 wk of age, seminiferous tubules contained Sertoli cells and early pachytene spermatocytes, which are the most mature cells of the germ cell lineage. One week later, early spermatids largely populated the tubules, and differentiating elongated spermatids were first detected at P28. At P60, when the animals are adults, spermatogenesis was cyclic and could be divided into 12 stages (I–XII) based on the morphological transformation of spermatids into spermatozoa in a process referred as spermiogenesis [26].

The first signs of disorganization in *Cldn11*^{-/-} testes appeared at P20 (Fig. 1, A, B, D, and E) and were obvious by P28. Indeed, when compared to the well-organized epithelium in the first wave of spermatogenesis from control testes (Fig. 1G), germ cells in *Cldn11*^{-/-} testes appear abnormally localized. Round clusters of cells were observed closely apposed to the base of the seminiferous epithelium, and the testis tubular lumen was poorly defined and was filled with round spermatids, with the acrosome labeled with PAS or cell clusters (Fig. 1H, arrows). Moreover, although elongated spermatids appeared in some tubules of P28 control testes (Fig. 1G), only scarce ectopically localized round spermatids were present in *Cldn11*^{-/-} testes (Fig. 1H). In addition, elongated spermatids were never observed in *Cldn11*^{-/-} testes at P28 or P60, and spermatogenesis did not proceed through the complete process of germ cell differentiation, which is consistent with published findings [19]. The phenotype was accentuated at P60 (Fig. 1, J and K), and PAS-positive material was observed inside the cell clusters (Fig. 1K, arrows), indicative of the presence of glycoproteins.

We next compared the temporal appearance of the *Cldn11*^{-/-} testis phenotype with that of protein expression in control testes (Fig. 1, C, F, and I). Although claudin 11 was not detected by immunohistochemistry at P10 (data not shown), it was obvious in some tubules at P13 in testes from wild-type animals, with labeling extending from the basal membrane to the lumen (Fig. 1C). Such staining is consistent with the localization of claudin 11 to plasma membrane and the polarization of Sertoli cells from P20 onward (Fig. 1, F and I). In time-matched *Cldn11*^{-/-} testes, no labeling was observed, thus confirming the specificity of the antibody (Supplemental Fig. S1; all Supplemental Data are available online at www.biolreprod.org). Testis weight in *Cldn11*^{-/-} mice was normal up to P28 (Fig. 1L).

Cell Clusters Comprise Sertoli Cells

Histological sections reveal that nuclei from the vast majority of cells in adluminal cell clusters are clear and contain one to three nucleoli, which is reminiscent of normal Sertoli cell morphology (data not shown). However, in P60 *Cldn11*^{-/-} testes, mixed cell nuclei are observed in the clusters (data not shown and Gow et al. [19]). To identify the cells comprising these clusters, we performed immunohistochemis-

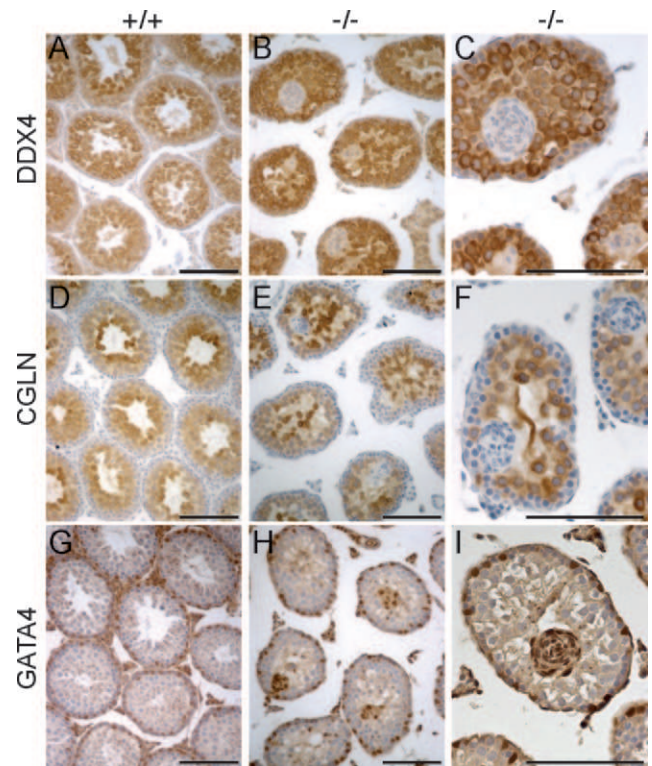


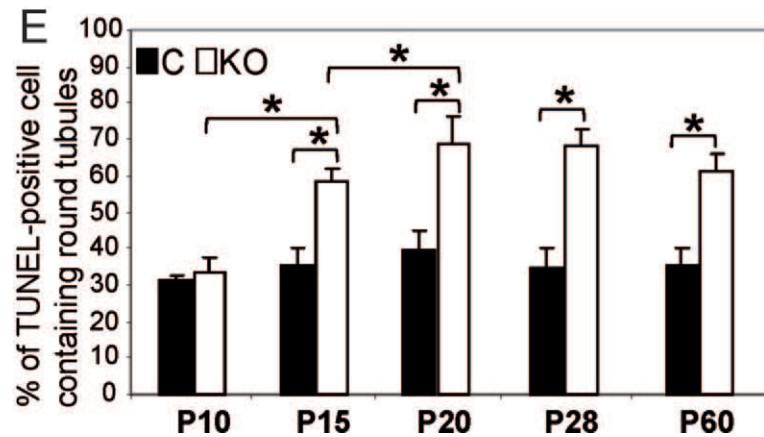
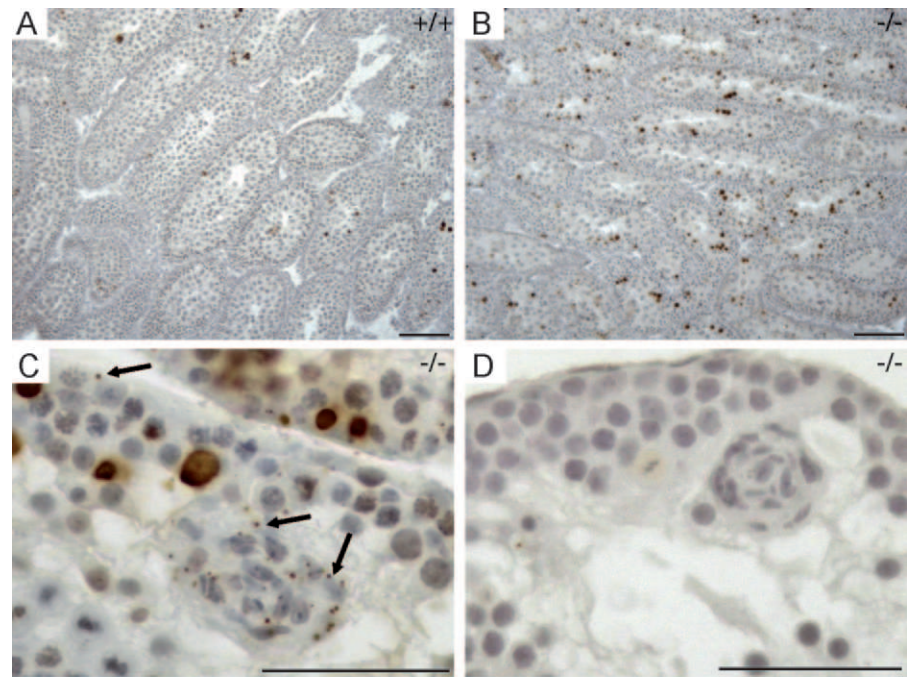
FIG. 2. Nature of cell clusters. Immunolabeling of germ cell markers DDX4 (A–C) and calmegein (CLGN), recognized by the TRA369 antibody (D–F), and Sertoli cell marker GATA4 (G–I) of P28 control (A, D, and G) and *Cldn11*^{-/-} (B, C, E, F, H, and I) testes show that cell clusters found in the lumen of *Cldn11*^{-/-} testes comprise Sertoli cells. Bars = 100 μ m.

try for several germ cell markers (Fig. 2): the DDX4 protein (mouse vasa homolog) is expressed from zygotene spermatocytes to round spermatids (Fig. 2A) [27–29]; Calmegein (CLGN) is expressed in early pachytene spermatocytes to step 14 spermatids (Fig. 2D) [30, 31]; and vitronectin [32] and claudin 1 (data not shown) are expressed in the acrosomes of spermatids. The absence of these markers demonstrates that cell clusters in *Cldn11*^{-/-} seminiferous tubules do not contain germ cells (Fig. 2, B, C, E, and F, and data not shown), although we occasionally observed a few germ cells in some cell clusters from P60–P180 mice (data not shown). Immunolabeling of GATA4, which identifies Sertoli cells inside the seminiferous epithelium (Fig. 2G) [33, 34], clearly indicated that clusters comprise Sertoli cells (Fig. 2, H and I).

Increased Apoptosis in Testis of *Cldn11*^{-/-} Mice

Although claudin 11 expression in testis is Sertoli cell specific, the primary defect in *Cldn11*^{-/-} mice is that of a failure of spermatogenesis. Apoptosis is the dominant pathway for eliminating germ cells whenever the supporting Sertoli cells are unable to provide a supportive environment for their development [35]; thus, we characterized the fate of germ cells by using TUNEL labeling (Fig. 3). Quantification of TUNEL-labeled cells in *Cldn11*^{-/-} testis showed a significant ($P < 0.05$) increase in the incidence of apoptosis at P20 and P28 compared with age-matched controls (Fig. 3). The proportion of round tubules containing one or more TUNEL-positive cells was increased 1.5-fold ($P < 0.05$) in *Cldn11*^{-/-} testes at P15 (Fig. 3E), suggesting an early impact of the absence of claudin 11 on germ cell development. Apoptosis reached a peak at P20 and was maintained through P28, but it remained elevated at

FIG. 3 High incidence of germ cell apoptosis in *Cldn11*^{-/-} testes. TUNEL analysis of control (A) and *Cldn11*^{-/-} (B and D) testes at P20 (A and B) shows increased germ cell apoptosis in *Cldn11*^{-/-} testes. In addition to TUNEL-positive germ cells localized in the seminiferous epithelium, small vesicles of fragmented TUNEL-positive DNA reminiscent of phagocytosis are abundant in cytoplasm of sloughing Sertoli cells (arrows in C) and absent in control TUNEL analysis (D). In E, counts of round seminiferous tubules containing at least one TUNEL-positive cell. Data show that first significant increase was seen at P15. Values are mean \pm SEM of three to six animals. Asterisks indicate statistical significance ($P < 0.001$) by one-way ANOVA followed by Holm-Sidak posthoc testing. Bars = 100 μ m (A and B) and 50 μ m (C and D).



P60 and was not statistically different from levels at P20. In addition, abundant vesicles of fragmented TUNEL positive-DNA were detected in the cytoplasm of sloughing Sertoli cells (Fig. 3C, arrows), which likely indicates that Sertoli cells phagocytose degenerating germ cells. These kinetics are consistent with the notion that germ cell progression through meiosis is impeded in the absence of Sertoli cell TJs.

To further dissect the fate of germ cells in *Cldn11*^{-/-} testes, sections were immunostained with phosphorylated histone H3 (Ph-H3; Fig. 4). Phosphorylated histone H3 is normally expressed in mitotic spermatogonia and in diplotene spermatocytes approaching cell division at stages XI and XII [36]. Immunolabeling of Ph-H3 at P15, P28, and P60 showed no obvious changes in mitotic spermatogonia or meiotic spermatocytes (Fig. 4, A–F; small magnifications not shown) from the proportions of round tubules containing one or more Ph-H3-positive cells (Fig. 4G). By contrast, the number of Ph-H3-positive cells per round tubule increased from P28 to P60 in control testes but remained constant in *Cldn11*^{-/-} testes (Fig. 4, C–F and H). Consequently, the total number of Ph-H3-positive cells decreased in *Cldn11*^{-/-} testes (Fig. 4H) at P28 and P60. Together, these data suggest that the decrease of phospho-H3-labeled germ cell number may well result from the increase of germ cell apoptosis.

Dynamics of Sertoli Cell Sloughing in *Cldn11*^{-/-} Testes

To determine how a lack of claudin 11 might have an impact on Sertoli cell topography within the seminiferous epithelium, sections were immunolabeled with GATA4 (Fig. 5). In control testes, Sertoli cell nuclei were positioned at the basement membrane of the seminiferous epithelium, as expected. In *Cldn11*^{-/-} testes, the nuclei were localized toward the center of the tubule as early as P13 (Fig. 5, A and B), which coincided with the beginning of claudin 11 expression in control testes (Fig. 1C). At P28 (Fig. 5, C–F)—also seen at P20 (data not shown)—basally located Sertoli cells were observed, as were several abnormal Sertoli cell arrangements. These include groupings of Sertoli cells adjacent to the base of the tubule (Fig. 5D), round clusters with few cells attached to the basement membrane (Fig. 5E), and completely detached Sertoli cell clusters filling the tubule lumen (Fig. 5F). These data are probably indicative of dynamic Sertoli cell sloughing from their basal sites into the lumen of the tubule. Consistent with our proposal that Sertoli cells are sloughed from the epithelium into the duct system is our observation that GATA4-positive cell clusters occur in the lumen of the epididymis of P60 *Cldn11*^{-/-} mice (Fig. 5G).

In this light, we hypothesize that Sertoli cells may migrate along the basement membrane to form small groups, which

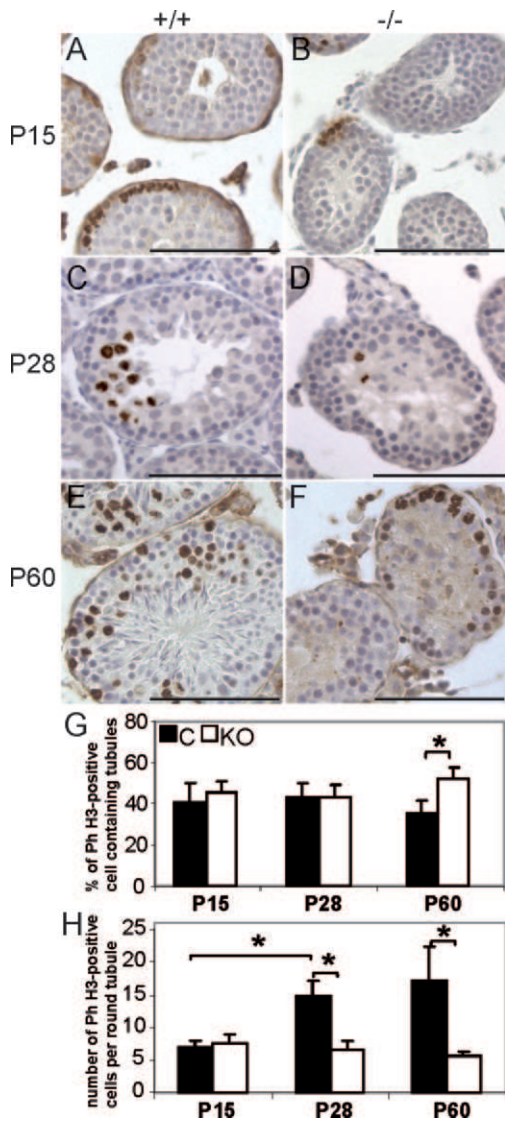


FIG. 4. Depletion of germ cells. Immunolabeling of phospho-H3 in primary spermatocytes of P15 (A and B), P28 (C and D), and P60 (E and F) control (A, C, and E) and *Cldn11*^{-/-} (B, D, and F) testes show germ cells in the division phases. Analysis of the percentage of round tubules that contain at least one Ph-H3-positive cell (G) together with the number of Ph-H3-positive cells per round tubule (H) shows the progressive loss of germ cells. Asterisks indicate statistical significance ($P < 0.001$) by Mann-Whitney rank test (G) or Kruskal-Wallis one-way ANOVA followed by Dunn pairwise multiple-comparison testing (H). Bars = 100 μ m.

then detach, or they may form clusters by cell division and thereafter detach. To distinguish between these possibilities, we examined changes in the number of Gata4-labeled Sertoli cells from P15 to P60 (Fig. 6, A–C). Consistent with the temporal development of the phenotype, the number of Sertoli cells per cluster rose from P15 to P28 and was maintained at this level through P60 in *Cldn11*^{-/-} testes (Fig. 6A). In addition, the proportion of round tubules containing detached Sertoli cells almost doubled between P15 and P60 ($P < 0.05$). Indeed, more than 80% of the tubules contained Sertoli cell clusters at P60 (Fig. 6B).

Although the number of Sertoli cells per round tubule decreased from P15 to P60 in control testes (probably as a result of dilution due to a massive increase of the germ cell population within the tubules as the animals mature), the size of this population remained almost constant in *Cldn11*^{-/-} testes

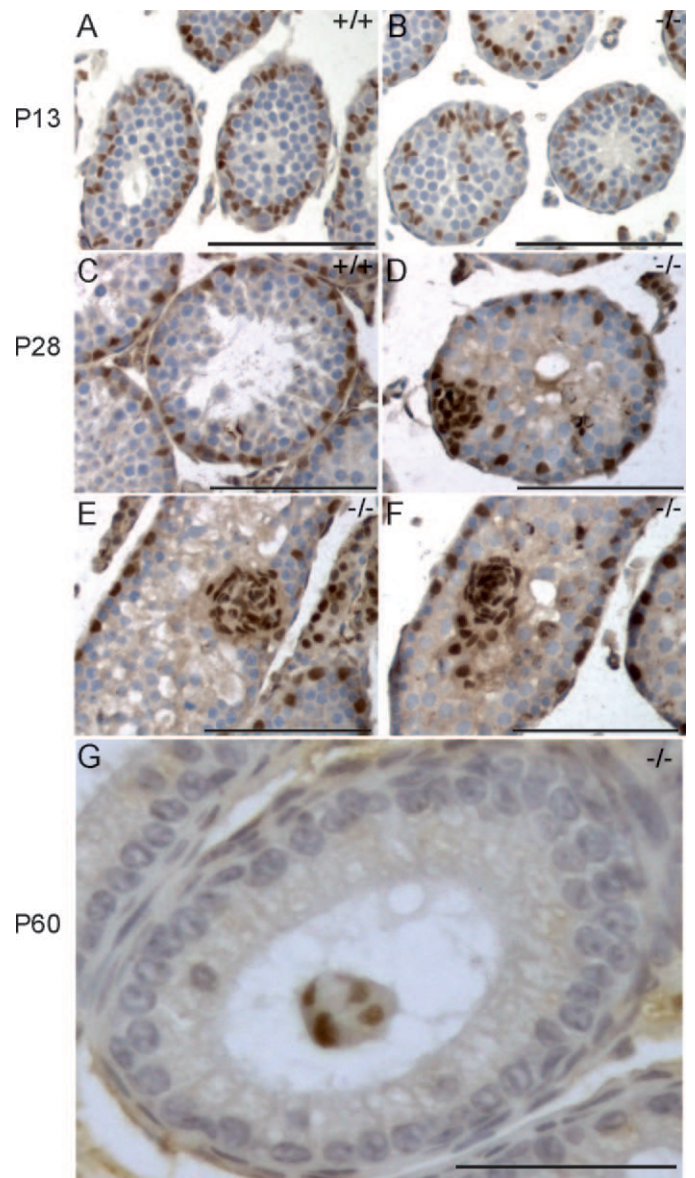


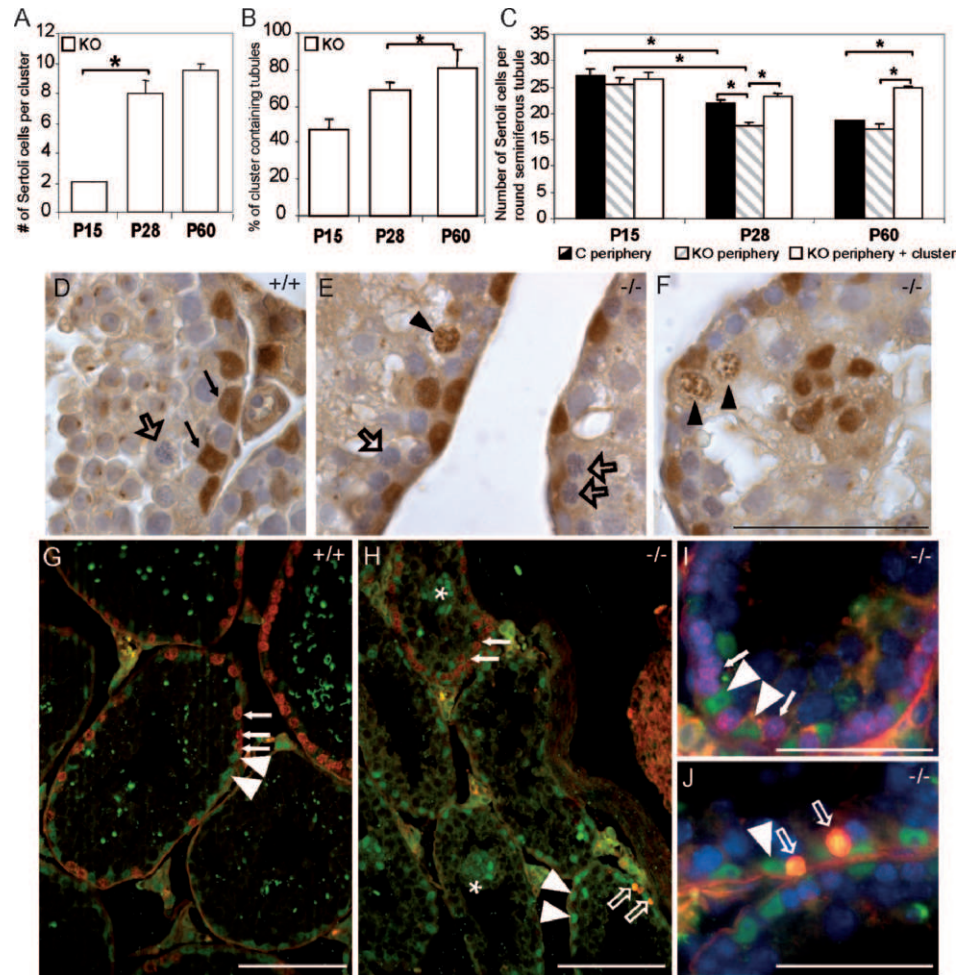
FIG. 5. Dynamics of Sertoli cell sloughing. Immunolabeling of GATA4 of P13 (A and B) and P28 (C–F) control (A and C) and *Cldn11*^{-/-} (B and D–F) testes shows the progressive sloughing of Sertoli cells from P13 onward and from the base (D) to the lumen (E and F) of the seminiferous tubule. Immunolabeling of GATA4 of P60 *Cldn11*^{-/-} epididymis (G) shows the presence of Sertoli cell clusters. Bars = 100 μ m (A–F) and 50 μ m (G).

(Fig. 6C). The number of Sertoli cells per round tubule in control and *Cldn11*^{-/-} testes was similar at P15 and at P28 if both peripherally located and cluster-located Sertoli cells are considered. At P60, the number of peripherally located Sertoli cells was similar in control and *Cldn11*^{-/-} testes but higher in *Cldn11*^{-/-} testes when considering total Sertoli cell numbers. Together, these data suggest a continuous renewal of Sertoli cells to compensate for their losses from detachment and shedding into the lumen.

Sertoli Cells Undergo Cell Division in *Cldn11*^{-/-} Testes

Sertoli cells cease dividing in immature animals during the first 2 wk after birth, which is concomitant with the appearance of meiotic germ cells and formation of the lumen [37, 38]. To determine the cell cycle status of Sertoli cells, we performed an

FIG. 6. Sertoli cell number evolution. Counts of GATA4-positive cells in round tubules show that both the number of Sertoli cells per cluster (A) and the percentage of seminiferous tubules that contain clusters (B) increase with age in *Cldn11*^{-/-} testes. The comparison of the number of Sertoli cells located at the periphery of control round tubules and with the total number of Sertoli cells located at the periphery of round tubule in *Cldn11*^{-/-} testes shows the relative maintenance of Sertoli cells at P28 and the relatively high total number of Sertoli cells at P60 (C). Asterisks indicate statistical significance ($P < 0.001$) by one-way ANOVA followed by Tukey posthoc testing. Close examination of Gata4 labeling of control (D) and *Cldn11*^{-/-} (E and F) testis sections at P28 (D–F) show the chromatin aspect of GATA4-labeled Sertoli cell nuclei, from dense compact (solid arrows) to heterogeneous (arrowheads), compared with the compacted chromatin of meiotic spermatocytes (large open arrows). Double labeling of Gata4-positive Sertoli cells (green; arrowheads) and BrdU-positive dividing cells (red) in control (G) and *Cldn11*^{-/-} (H and J) P28 testes show the presence of double-labeled dividing Sertoli cells (open arrows), compared with dividing germ cells (solid arrows). Asterisks depict GATA4-positive Sertoli cell clusters. High magnifications of GATA4-labeled (green) and BrdU-labeled (red) cells and nuclei (blue) in *Cldn11*^{-/-} P28 testis are shown in I and J. Bars = 50 μ m (D–F, I, and J) and 100 μ m (G and H).



in-depth survey of GATA4-labeled Sertoli cells (Fig. 6, D–F). In control testes, GATA4 labeling of Sertoli cell nuclei was homogenous, with the exception of nucleoli (Fig. 6D, arrows), and similarly labeled Sertoli cells were found in P28 (Fig. 6, E and F) and P60 (data not shown) *Cldn11*^{-/-} testes. In addition, heterogeneous chromatin in GATA4-positive nuclei was also observed (Fig. 6, E and F, arrowheads), together with the characteristic meiotic figures of germ cells (Fig. 6E, arrows).

Juxtaposed Sertoli cells in the plane parallel to the basement membrane in *Cldn11*^{-/-} testes (Fig. 6E) suggest that this cell population may be dividing. To identify dividing Sertoli cells, we used *in vivo* BrdU incorporation prior to the fixation and tissue processing (Fig. 6, G–J). Comparison of the Gata4-positive Sertoli cell and BrdU-positive dividing cell populations in wild type testes reveals the canonical complementary pattern of Sertoli cell and spermatogonia (Fig. 6G). This is a hallmark of stage VIII tubules, wherein spermatogonia proliferate and leptotene spermatocytes traverse the BTB into the adluminal compartment for further development [12, 27, 29, 32]. In *Cldn11*^{-/-} testes, stage VIII tubules contained Gata4-positive Sertoli cells (Fig. 6, H–J, arrowheads) and BrdU-labeled spermatogonia (Fig. 6, H and I, solid arrows), indicating that the lack of claudin 11 expression does not hamper the spermatogenic cycle, or at least the cyclical entry of spermatogonia into mitosis at stage VIII [26]. However, we also observed double-labeled cells at the periphery of some tubules (Fig. 6, H and J, open arrows), which demonstrates that Sertoli cells are proliferating in *Cldn11*^{-/-} testes. These double-labeled Sertoli cells, however, were found at a

frequency of one to three per testis section, mostly grouped in one tubule, suggesting that the rate of Sertoli cell proliferation is probably low. Importantly, we did not observe BrdU labeling of cell clusters. It may indicate that Sertoli cell division occurs prior to cluster formation and shedding into the lumen.

Loss of Sertoli Cell Polarity but Maintenance of Differentiation Markers

In Figure 5, we observe that Sertoli cells in *Cldn11*^{-/-} testes changed shape in the course of cell cluster sloughing. Thus, the nuclei of basal Gata4-labeled Sertoli cells were round or triangular, whereas Sertoli cells located at the periphery of clusters had round nuclei, and those within clusters had smaller and elongated or comma-shaped nuclei. Such shapes are reminiscent of fibroblasts (Fig. 7A) and indicate a loss of cell polarity, and possibly differentiation status. To examine these possibilities, we analyzed several Sertoli cell differentiation markers. Vimentin, androgen receptor, and N-cadherin labeling (Fig. 7, B–E, H, and I; and data not shown) demonstrated that *Cldn11*^{-/-} Sertoli cells retain mature markers, even in luminal cell clusters from P180 testes when the number of germ cells and, consequently, testis weight is in decline. We also observed vimentin-positive Sertoli cell clusters in the epididymides of *Cldn11*^{-/-} mice (Fig. 7, F and G), probably suggesting that they are cleared from the testes in a fashion similar to sperm cells. Consistent with the absence of sperm, the lumen of most epididymides were empty (Fig. 7G). By

contrast, epididymides from control animals were filled with sperm cells (Fig. 7F).

Molecular Characterization of *Cldn11*^{-/-} Testes Using Microarrays

To better understand the molecular consequences of the absence of claudin 11 on Sertoli cells, we performed a microarray analysis of whole-testis mRNA from P20 *Cldn11*^{-/-} mice. Littermate *Cldn11*^{+/-} mice were used as controls, which are fertile and otherwise indistinguishable from wild-type mice in all studies we have performed. The choice of P20 stems from two main considerations; testis weight and germ cell composition are similar in *Cldn11*^{-/-} and control groups, and Sertoli cells detached from the basement membrane can be observed. The strategy was based on a subtractive approach following a dye swap experimental procedure to catch the most differentially upregulated and downregulated genes. Microarray analysis identified 108 genes significantly upregulated and 98 downregulated by more than 1.3-fold in *Cldn11*^{+/-} compared with *Cldn11*^{-/-} testes (SAM procedure with a false discovery rate <5%). Importantly, *Cldn11* was the most downregulated gene (Table 2), which accords with the genotype of *Cldn11*^{-/-} mice. In addition, we selected six upregulated genes and one downregulated gene on the basis of the amount of expression and their possible biological significance and confirmed differences in the expression levels by quantitative PCR analysis (Table 2). In agreement with the histological data (Fig. 1, D and E), among the upregulated genes, 22 (20.4%) were inferred to Sertoli cells and four (3.7%) to germ cells; among the downregulated genes, 28 (29.6%) were inferred to germ cells, most often spermatocytes (Supplemental Table S1). Also consistent with the immunohistological data, the *Vim* gene was already upregulated in P20 *Cldn11*^{-/-} testes. Interestingly, typical Sertoli cell markers, such as ETV5 (also known as ERM), SOX8, SOX9, Desert hedgehog, transferrin, GJA1 (connexin 43), or Kit ligand, displayed a similar expression in control and *Cldn11*^{-/-} testes (data not shown). Notably, WebGestalt analysis of microarray data revealed a statistical enrichment of TJ ($P = 1.36 \cdot 10^{-6}$), regulation of actin cytoskeleton ($P = 2.72 \cdot 10^{-3}$), cell cycle ($P = 1.14 \cdot 10^{-4}$), glutathione metabolism ($P = 2.75 \cdot 10^{-7}$), and adherens junction ($P = 1.84 \cdot 10^{-3}$) KEGG pathways. Interestingly, expression of genes of the tight and adherens junctions and actin and intermediate filament cytoskeleton pathways were coordinately upregulated (16 of 18 genes and 14 of 15 genes, respectively).

DISCUSSION

The present data highlight the critical role of claudin 11 in the maintenance of Sertoli cell epithelial differentiation. Indeed, in the absence of claudin 11, Sertoli cells differentiate, can proliferate, and are not permanently arrested as nonmitotic quiescent cells. Thus, Sertoli cells can exhibit one feature of an immature cell without reverting to the state of immaturity. They form homogeneous clusters, lose their contact with basement membrane, detach from the seminiferous epithelium, and acquire a fibroblastlike cell shape. At the molecular level, the absence of claudin 11 expression is associated with selective changes in several cell junction-related genes, specifically TJ genes, as well as cytoskeleton-related genes.

A growing number of genes associated with male infertility have been generated using homologous recombination in embryonic stem cells [39, 40]. A frequent feature of mouse models of infertility is germ cell defect consecutive to either

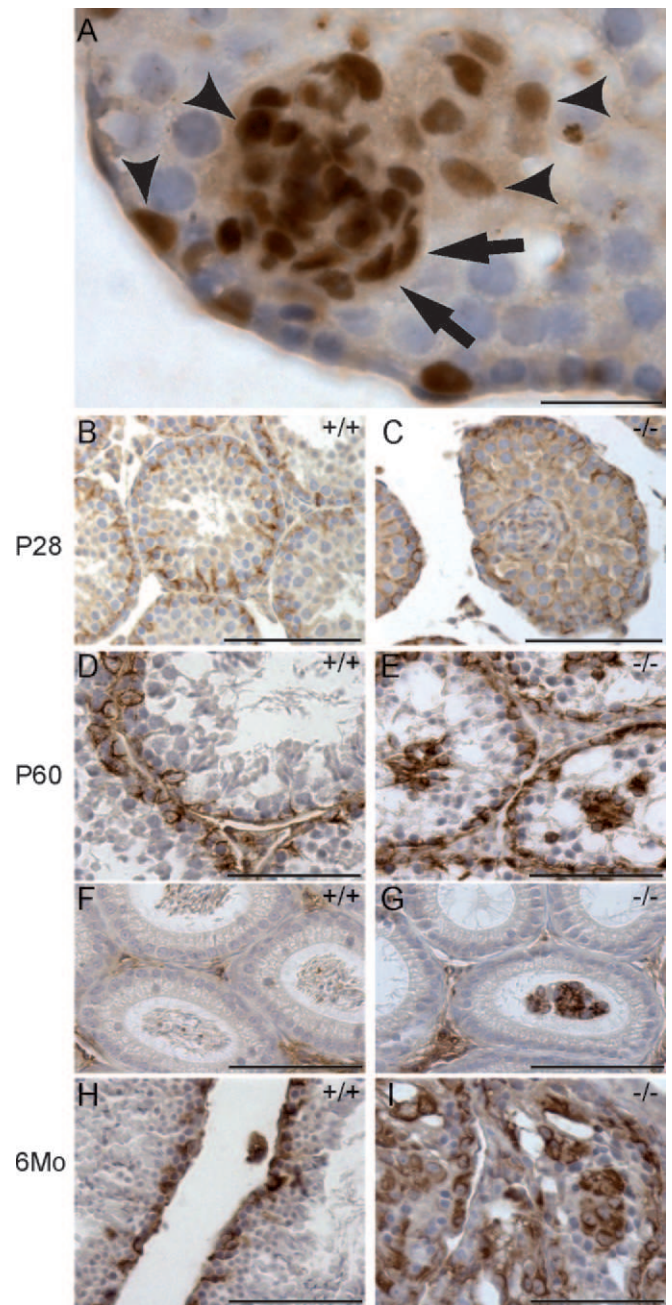


FIG. 7. Sertoli cell loss of polarity. Immunolabeling of GATA4 in Sertoli cell nuclei of P28 (A) *Cldn11*^{-/-} testes shows the progressive change in Sertoli nuclei shape, from round (arrowhead) to fibroblastlike elongated (arrows). Immunolabeling of vimentin in Sertoli cells of P28 (B and C), P60 (D–G), and 6-mo (H and I) control (B, D, F, and H) and *Cldn11*^{-/-} (C, E, G, and I) testes (B–E and H–I) and epididymides (F and G) shows the maintenance of vimentin expression in detached Sertoli cell clusters from the seminiferous tubule to the epididymis lumen in *Cldn11*^{-/-} animals. Bars = 20 μ m (A) and 100 μ m (B–I).

depletion of stem cells, meiosis arrest, or spermiogenesis default. Disruption of meiosis notably induces massive germ cell apoptosis and elimination by their phagocytosis by Sertoli cells, resulting in such histological characteristics as vacuoles in Sertoli cell cytoplasm and multinucleated spermatids. As well, the primary impact of somatic cell physiology disruption (very often through impairment of hormonal action) is germ cell development damage. By comparison, ablation of genes encoding TJ proteins, such as occludin (*Ocln*), ZO-1 (*Tjp1*),

TABLE 2. List of selected up- and down-regulated genes in P20 *Cldn11*^{-/-} testes.

Gene product	Gene symbol	Accession no.	Microarray fold change	Q _t PCR fold change
Tight and adherens junctions				
Metadherin	<i>Mtdh</i>	NM_026002	+1.60	+1.09*
Solute carrier family 35, member F2	<i>Slc35f2</i>	NM_028060	+1.58	
Proto-oncogene tyrosine-protein kinase FYN	<i>Fyn</i>	NM_008054	+1.55	+1.27*
Espin	<i>Espn</i>	NM_019585	+1.51	+1.42*
Src-substrate cortactin	<i>Cttn</i>	NM_007803	+1.51	
Cingulin-like 1	<i>Cgln1</i>	NM_026599	+1.42	
Ras homolog gene family member U	<i>Rhou</i>	NM_133955	+1.38	
Exocyst complex component 4 (Sec811)	<i>Exoc4</i>	NM_009148	+1.34	+1.22
Ras related protein Rab-12	<i>Rab12</i>	NM_024448	+1.34	
Junctional adhesion molecule 1 (JAM-A)	<i>F11r</i>	NM_172647	+1.33	
Vinculin	<i>Vcl</i>	NM_009502	+1.31	
Spectrin alpha 2 (fodrin)	<i>Spnb2</i>	NM_175836	+1.29	
Protein kinase C, delta type	<i>Prkcd</i>	NM_011103	+1.24	
Rho GTPase-activating protein	<i>Grit</i>	NM_177379	+1.22	
Alpha actinin 4	<i>Actn4</i>	NM_021895	+1.17	
Cold shock domain protein A	<i>Csda</i>	NM_011733	-1.56	-1.52*
Claudin 11	<i>Cldn11</i>	NM_008770	-2.13	
Tight junction protein 1 (ZO-1)	<i>Tjp1</i>	NM_009386		+1.92*
Actin or intermediate filament cytoskeleton				
Gelsolin	<i>Gsn</i>	NM_146120	+1.57	
Actin-related protein 2/3 complex, subunit 1B	<i>Arpc1b</i>	NM_023142	+1.55 / +1.36	
Vimentin	<i>Vim</i>	NM_011701	+1.44	
Thymosin beta 4X chromosome	<i>Tmsb4x</i>	NM_021278	+1.38	
Actin-related protein 2/3 complex, subunit 5	<i>Arpc5</i>	NM_026369	+1.37	
Plastin 3 (T-isoform)	<i>Pls3</i>	NM_145629	+1.35	
Tyrosine 3-monooxygenase/tryptophan 5-monooxygenase activation protein, eta polypeptide (14-3-3 eta)	<i>Ywhah</i>	NM_011738	+1.32	
Cytoplasmic FMR1 interacting protein 1 (Sra-1)	<i>Cytip1</i>	NM_011370	+1.30	
Dystroglycan 1	<i>Dag1</i>	NM_010017	+1.30	
LIM and SH3 protein 1	<i>Lasp1</i>	NM_010688	+1.29	+1.59*
14-3-3 protein alpha/beta	<i>Ywhab</i>	NM_018753	+1.28	
Pleckstrin homology domain containing, family H (with MyTH4 domain) member 2	<i>Plekhh2</i>	NM_177606	+1.28	
Actin-like protein 6A	<i>Actl6a</i>	NM_023402	+1.24	
Myosin light chain regulatory B	<i>Mylc2b</i>	NM_023402	+1.22	
Actin-like-7-beta	<i>Actl7b</i>	NM_025271	-1.36	

* Statistical significance ($P < 0.005$) in P20 *Cldn11*^{-/-} testes versus time-matched wild-type testes.

and *F11r*, displays variable phenotypes, ranging from Sertoli cell-only syndrome of the old adult to the apparent absence of a testicular phenotype [15, 18, 41]. Together, our results demonstrate that claudin 11 plays a key role in both Sertoli cell physiology and spermatogenesis.

Sertoli cell clusters have been described previously in several mouse models of infertility consecutive to germ cell loss [42, 43]. Among them, very few involve a primary defect in the Sertoli cell maturation process (i.e., proliferation and differentiation), and none of them result in the uncoupling between these two states. For example, delayed Sertoli cell cluster formation has been reported in adult *Dazl*^{-/-} mice, where the primary defect is a failure of stem spermatogonia to differentiate into spermatogonia committed to spermatogenesis [43], and in rats treated with busulphan, which interferes with germ cell renewal [42, 43]. In mice with a Sertoli cell-specific gene ablation of *Gjal* (also called Connexin43), continued Sertoli cell proliferation in adulthood and clusters of sloughed cells comprising Sertoli cells have been observed. However, Sertoli cell sloughing is concurrent with a dramatic early depletion of germ cells, and Sertoli cell differentiation is inhibited [17, 44]. By contrast, Sertoli cell disorganization in *Cldn11*^{-/-} testes is conspicuous from P13, when there is little evidence of germ cell pathology or apoptosis. At P20, tubules are filled with germ cells, and germ cell depletion is not

obvious until germ cells fail to progress beyond meiosis. Consequently, Sertoli cell detachment may be a primary defect of *Cldn11*^{-/-} testes, and the lack of claudin 11 does not preclude maturation of Sertoli cells, as shown in the microarray study.

Several lines of evidence indicate that claudin 11 expression and TJ permeability are directly regulated by androgen signaling. Adult mice that are deficient for androgen receptor only in Sertoli cells (S-AR^{-ly}) display Sertoli cell disorganization similar to that observed in *Cldn11*^{-/-} mice. This is associated with a sharp decrease in *Cldn11*, *Ocln*, and *Gsn* mRNA levels, as well as an increase in *Vim* expression [45]. Mice expressing a mutant form of the androgen receptor display abnormal expression of TJ proteins and Sertoli cell cytoskeleton genes [44]. Detachment of Sertoli cells has been reported in antiandrogen cimetidine-treated rats [46]. Collectively, these in vivo mouse models support the physiological relevance of in vitro demonstrations that claudin 11 expression is regulated by androgens [47].

In contrast to cimetidine-treated rats, in which Sertoli cell detachment from the basement membrane parallels Sertoli cell apoptosis [46], claudin 11 deficiency is associated with Sertoli cell proliferation and germ cell apoptosis and phagocytosis. Microarray data from these animals reveal an induction of detoxification machinery in Sertoli cells (upregulation of

Gstm1 and *Gstm6* [48, 49]) and a suppression of detoxification machinery in germ cells (downregulation of *Gstm3* [50]). It is tempting to speculate that these changes may constitute an initial trigger for germ cell apoptosis. Tight junctions are critical regulators of the microenvironment in epithelia and determine paracellular barrier properties. Because claudin 11 forms TJs by itself [51–53], its loss disrupts Sertoli cell TJs and perturbs the seminiferous epithelium microenvironment. This is analogous to previous studies showing that germ cell apoptosis is an indirect effect of a leaky BTB caused by the absence of a protease inhibitor [32].

Alternatively, germ cell apoptosis may occur concurrently with an intrinsic Sertoli cell defect. This is similar to a loss of fetal androgen, which disrupts Sertoli cell maturation and impedes the ability of these cells to protect germ cells [54]. Phagocytosing Sertoli cells generate large amounts of free radicals [55], which is compensated by induction of antioxidant pathways. However, germ cells are poorly equipped to combat free radical attack and are particularly vulnerable because their plasma membrane is rich in polyunsaturated fatty acids [55, 56]. Oxidative stress has been linked to apoptosis [57]; thus, it could be hypothesized that excessive germ cell phagocytosis by Sertoli cells itself induces the Sertoli cell to produce free radicals that will provoke apoptosis of surviving neighboring germ cells. However, the two hypotheses do not exclude each other.

In light of the possibility that the Sertoli cell phenotype stems directly from claudin 11 deficiency, we hypothesize that one mechanism may involve Sertoli cell proliferation. During development, mouse Sertoli cells normally stop dividing commensurately with assembly of the BTB and the beginning of spermatogenesis. This leads to an almost quiescent state during the second week of life in mice [37, 38, 58]. In vitro, recent studies show that P7–P8 and adult mouse Sertoli cells can resume mitosis, and that this phenomenon is accentuated by the absence of connexin43, suggesting that Sertoli cells may be arrested proliferative cells rather than terminally differentiated somatic cells [59, 60]. In the current study, we observe that some Sertoli cells lacking claudin 11 in vivo incorporate BrdU at P28 and P60, thereby demonstrating that they can proliferate, albeit at a low proliferation rate. Nevertheless, Sertoli cell number in *Cldn11*^{-/-} mice is comparable to controls at P28 and slightly increased at P60. Additionally, Sertoli cells are still present in 6-mo-old *Cldn11*^{-/-} testes, despite their continuous sloughing from the epithelium.

Interestingly, functional TJs assemble when Sertoli cells cease to divide, which suggests that BTB formation could regulate Sertoli cell cycle. Consistent with this notion, the upregulation of cell cycle genes observed in the microarray data is partially attributable to Sertoli cell proliferation rather than only to germ cells committed to apoptosis. Indeed, among cell cycle upregulated genes, *Rab12* is expressed by Sertoli cells, whereas *Cdk5* is germ cell specific [61, 62]. Downregulated cell cycle genes in *Cldn11*^{-/-} testes, including *Ccnb2* and *Ccna1*, have mostly been described in meiotic germ cells [63, 64]. Thus, we hypothesize that the assembly of claudin 11 TJs helps to ensure that Sertoli cells are contact inhibited and remain quiescent.

In the current study, we find that the Sertoli cell phenotype in the seminiferous tubules of *Cldn11*^{-/-} mice includes the acquisition of a fibroblastic cell shape in cell clusters. Changes in cell shape are often associated with altered cytoskeletal gene expression, and it is satisfying that our microarray analysis reveals a number of changes in the expression of Sertoli cell-specific genes, including *Vcl*, *Actn4*, *Spna2*, and *Vim*.

Conceivably, the induction of these genes may be related to a germ cell apoptosis-related shift in the composition of the epithelium; however, several canonical Sertoli cell markers are unchanged, which argues against a significant change in the Sertoli cell:germ cell ratio. Although dedifferentiation of Sertoli cells might be an expected outcome of persistent proliferation and reorganization of the vimentin network, our microarray data show that these cells maintain the expression of several mature Sertoli cell markers, including *Gata1* and *Fshr* [65], at P20. Therefore, we find no evidence that Sertoli cells are committed to a dedifferentiation process in the absence of TJs.

Alternatively, Sertoli cells could become committed to a preneoplastic process in the absence of TJs. In addition to Sertoli cell proliferation, *Cldn11*^{-/-} testes express high levels of *Mtdh*, which is a known tumor cell marker [66]. However, dividing Sertoli cells are scarce and only observed at the periphery of tubules, and not in luminal cell clusters, which would indicate that these cells become quiescent before they slough. Moreover, instead of invading the entire testis, Sertoli cell clusters are cleared via the normal conducts and are found in the epididymis. At 6 mo, testis histology is not significantly different from that at 2 mo, but it is dramatically different from typical Sertoli cell tumors [67, 68]. Finally, testicular tumors have not been observed in our mouse colony in more than 10 yr, despite maintaining mice beyond 12 mo of age (Gow, unpublished results). Although several studies have demonstrated the induction or suppression of various claudin genes in different cancers, in support of a relationship between TJ-based barrier function and cell proliferation [51–53], and our data strongly suggest that the absence of claudin 11 in Sertoli cells does not commit these cells to a neoplastic transformation. In addition, although more than one claudin family member has been shown at the BTB [69], we demonstrate a lack of functional redundancy at the BTB.

It is interesting that *Clu* was the most highly stimulated gene in our microarray study. Indeed, its encoded protein is known to cause aggregation of Sertoli cells from immature rats and TM-4 cells from mouse testis [70]. Aggregation of these cells is the first sign of fetal testis differentiation [71], but this behavior is probably independent of claudin 11 expression, because testis development and morphology at P10 are normal in *Cldn11*^{-/-} mice. Although mechanisms regulating homophilic recognition and cell aggregation in Sertoli cells are unclear, changes in expression of intercellular junction and cytoskeletal genes from our microarrays suggest a role for claudin 11 in intracellular signaling, including a feedback loop for the cell to compensate for excessive TJ permeability. Regulation of adherens junction proteins, such as N-cadherin (data not shown), may be sufficient for Sertoli cell aggregation, with claudin 11 mediating polarization. In addition, induction of the actin and intermediate filament genes may be related to the Sertoli cell shape changes and their sloughing into the lumen.

Among mouse models of male infertility, *Cldn11*^{-/-} mice display a unique testis phenotype in which the primary defect is epithelial disorganization, mitosis, and detachment of Sertoli cells from the basement membrane in the face of adult differentiation marker expression. Components of TJs directly influence signaling pathways and regulate epithelial differentiation and proliferation [72, 73]. To further dissect the role of claudin 11 at TJs between Sertoli cells, it would be of great interest to track the incidence of *Cldn11* knockdown on purified Sertoli cells, both at the phenotypic and transcriptome levels. Then, it would be possible to identify the genes that

show the highest degree of upregulation or downregulation, and the putative canonical pathways that might be affected by claudin 11.

ACKNOWLEDGMENTS

We thank Drs. T. Noce and H. Tanaka for providing for DDX4 and CGLN antibodies, respectively. We thank Mr. Kevin Olson, Center for Molecular Medicine and Genetics, Wayne State University, for technical assistance in the collection of tissues from the claudin 11 mouse colony.

REFERENCES

- Gumbiner BM. Breaking through the tight junction barrier. *J Cell Biol* 1993; 123:1631–1633.
- Schneeberger EE, Lynch RD. The tight junction: a multifunctional complex. *Am J Physiol Cell Physiol* 2004; 286:C1213–C1228.
- Dym M, Fawcett DW. The blood-testis barrier in the rat and the physiological compartmentation of the seminiferous epithelium. *Biol Reprod* 1970; 3:308–326.
- Flickinger C, Fawcett DW. The junctional specializations of Sertoli cells in the seminiferous epithelium. *Anat Rec* 1967; 158:207–221.
- Nicander L. An electron microscopical study of cell contacts in the seminiferous tubules of some mammals. *Z Zellforsch Mikrosk Anat* 1967; 83:375–397.
- Russell L. Observations on rat Sertoli ectoplasmic ('junctional') specializations in their association with germ cells of the rat testis. *Tissue Cell* 1977; 9:475–498.
- Brokelmann J. Fine structure of germ cells and Sertoli cells during the cycle of the seminiferous epithelium in the rat. *Z Zellforsch Mikrosk Anat* 1963; 59:820–850.
- Masri BA, Russell LD, Vogl AW. Distribution of actin in spermatids and adjacent Sertoli cell regions of the rat. *Anat Rec* 1987; 218:20–26.
- Romrell LJ, Ross MH. Characterization of Sertoli cell-germ cell junctional specializations in dissociated testicular cells. *Anat Rec* 1979; 193:23–41.
- Russell LD, Goh JC, Rashed RM, Vogl AW. The consequences of actin disruption at Sertoli ectoplasmic specialization sites facing spermatids after in vivo exposure of rat testis to cytochalasin D. *Biol Reprod* 1988; 39:105–118.
- Vogl AW, Grove BD, Lew GJ. Distribution of actin in Sertoli cell ectoplasmic specializations and associated spermatids in the ground squirrel testis. *Anat Rec* 1986; 215:331–341.
- Vogl AW, Pfeiffer DC, Mulholland D, Kimel G, Guttman J. Unique and multifunctional adhesion junctions in the testis: ectoplasmic specializations. *Arch Histol Cytol* 2000; 63:1–15.
- Vogl AW, Soucy LJ. Arrangement and possible function of actin filament bundles in ectoplasmic specializations of ground squirrel Sertoli cells. *J Cell Biol* 1985; 100:814–825.
- Weber JE, Turner TT, Tung KS, Russell LD. Effects of cytochalasin D on the integrity of the Sertoli cell (blood-testis) barrier. *Am J Anat* 1988; 182:130–147.
- Lui WY, Cheng CY. Regulation of cell junction dynamics by cytokines in the testis: a molecular and biochemical perspective. *Cytokine Growth Factor Rev* 2007; 18:299–311.
- Mirza M, Petersen C, Nordqvist K, Sollerbrant K. Coxsackievirus and adenovirus receptor is up-regulated in migratory germ cells during passage of the blood-testis barrier. *Endocrinology* 2007; 148:5459–5469.
- Cooke VG, Naik MU, Naik UP. Fibroblast growth factor-2 failed to induce angiogenesis in junctional adhesion molecule-A-deficient mice. *Arterioscler Thromb Vasc Biol* 2006; 26:2005–2011.
- Saitou M, Furuse M, Sasaki H, Schulzke JD, Fromm M, Takano H, Noda T, Tsukita S. Complex phenotype of mice lacking occludin, a component of tight junction strands. *Mol Biol Cell* 2000; 11:4131–4142.
- Gow A, Southwood CM, Li JS, Pariati M, Riordan GP, Brodie SE, Danias J, Bronstein JM, Kachar B, Lazzarini RA. CNS myelin and sertoli cell tight junction strands are absent in *Osp/claudin-11* null mice. *Cell* 1999; 99:649–659.
- Devaux J, Gow A. Tight junctions potentiate the insulative properties of small CNS myelinated axons. *J Cell Biol* 2008; 183:909–921.
- Gow A, Davies C, Southwood CM, Frolenkov G, Chrustowski M, Ng L, Yamauchi D, Marcus DC, Kachar B. Deafness in Claudin 11-null mice reveals the critical contribution of basal cell tight junctions to stria vascularis function. *J Neurosci* 2004; 24:7051–7062.
- Wang E, Miller LD, Ohnmacht GA, Liu ET, Marincola FM. High-fidelity mRNA amplification for gene profiling. *Nat Biotechnol* 2000; 18:457–459.
- Churchill GA. Fundamentals of experimental design for cDNA microarrays. *Nat Genet* 2002; 32(suppl):490–495.
- Tusher VG, Tibshirani R, Chu G. Significance analysis of microarrays applied to the ionizing radiation response. *Proc Natl Acad Sci U S A* 2001; 98:5116–5121.
- Zhang B, Kirov S, Snoddy J. WebGestalt: an integrated system for exploring gene sets in various biological contexts. *Nucleic Acids Res* 2005; 33:W741–W748.
- Oakberg EF. Duration of spermatogenesis in the mouse and timing of stages of the cycle of the seminiferous epithelium. *Am J Anat* 1956; 99:507–516.
- Toyooka Y, Tsunekawa N, Takahashi Y, Matsui Y, Satoh M, Noce T. Expression and intracellular localization of mouse Vasa-homologue protein during germ cell development. *Mech Dev* 2000; 93:139–149.
- Fujiwara Y, Komiya T, Kawabata H, Sato M, Fujimoto H, Furusawa M, Noce T. Isolation of a DEAD-family protein gene that encodes a murine homolog of *Drosophila* vasa and its specific expression in germ cell lineage. *Proc Natl Acad Sci U S A* 1994; 91:12258–12262.
- Noce T, Fujiwara Y, Sezaki M, Fujimoto H, Higashinakagawa T. Expression of a mouse zinc finger protein gene in both spermatocytes and oocytes during meiosis. *Dev Biol* 1992; 153:356–367.
- Yoshinaga K, Tani I, Toshimori K. Molecular chaperone calnexin localization to the endoplasmic reticulum of meiotic and post-meiotic germ cells in the mouse testis. *Arch Histol Cytol* 1999; 62:283–293.
- Watanabe D, Sawada K, Koshimizu U, Kagawa T, Nishimune Y. Characterization of male meiotic germ cell-specific antigen (Meg 1) by monoclonal antibody TRA 369 in mice. *Mol Reprod Dev* 1992; 33:307–312.
- Le Magueresse-Battistoni B. Serine proteases and serine protease inhibitors in testicular physiology: the plasminogen activation system. *Reproduction* 2007; 134:721–729.
- Ketola I, Rahman N, Toppari J, Bielinska M, Porter-Tinge SB, Tapanainen JS, Huhtaniemi IT, Wilson DB, Heikinheimo M. Expression and regulation of transcription factors GATA-4 and GATA-6 in developing mouse testis. *Endocrinology* 1999; 140:1470–1480.
- Viger RS, Mertineit C, Trasler JM, Nemer M. Transcription factor GATA-4 is expressed in a sexually dimorphic pattern during mouse gonadal development and is a potent activator of the Mullerian inhibiting substance promoter. *Development* 1998; 125:2665–2675.
- Print CG, Loveland KL. Germ cell suicide: new insights into apoptosis during spermatogenesis. *Bioessays* 2000; 22:423–430.
- Cobb J, Miyaike M, Kikuchi A, Handel MA. Meiotic events at the centromeric heterochromatin: histone H3 phosphorylation, topoisomerase II alpha localization and chromosome condensation. *Chromosoma* 1999; 108:412–425.
- Kluin PM, Kramer MF, de Rooij DG. Proliferation of spermatogonia and Sertoli cells in maturing mice. *Anat Embryol (Berl)* 1984; 169:73–78.
- Vergouwen RP, Jacobs SG, Huiskamp R, Davids JA, de Rooij DG. Proliferative activity of gonocytes, Sertoli cells and interstitial cells during testicular development in mice. *J Reprod Fertil* 1991; 93:233–243.
- Cooke HJ, Saunders PT. Mouse models of male infertility. *Nat Rev Genet* 2002; 3:790–801.
- Toshimori K, Ito C, Maekawa M, Toyama Y, Suzuki-Toyota F, Saxena DK. Impairment of spermatogenesis leading to infertility. *Anat Sci Int* 2004; 79:101–111.
- Toyama Y, Maekawa M, Yuasa S. Ectoplasmic specializations in the Sertoli cell: new vistas based on genetic defects and testicular toxicology. *Anat Sci Int* 2003; 78:1–16.
- Kopecky M, Semecky V, Nachtigal P. Vimentin expression during altered spermatogenesis in rats. *Acta Histochem* 2005; 107:279–289.
- Schrans-Stassen BH, Saunders PT, Cooke HJ, de Rooij DG. Nature of the spermatogenic arrest in *Dazl*^{-/-} mice. *Biol Reprod* 2001; 65:771–776.
- Wang RS, Yeh S, Chen LM, Lin HY, Zhang C, Ni J, Wu CC, di Sant'Agnes PA, deMesy-Bentley KL, Tzeng CR, Chang C. Androgen receptor in sertoli cell is essential for germ cell nursery and junctional complex formation in mouse testes. *Endocrinology* 2006; 147:5624–5633.
- Yu Z, Dadgar N, Albertelli M, Scheller A, Albin RL, Robins DM, Lieberman AP. Abnormalities of germ cell maturation and sertoli cell cytoskeleton in androgen receptor 113 CAG knock-in mice reveal toxic effects of the mutant protein. *Am J Pathol* 2006; 168:195–204.
- Sasso-Cerri E, Cerri PS. Morphological evidences indicate that the interference of cimetidine on the peritubular components is responsible for detachment and apoptosis of Sertoli cells. *Reprod Biol Endocrinol* 2008; 6:18.
- Kaitu'u-Lino TJ, Sluka P, Foo CF, Stanton PG. Claudin-11 expression and localisation is regulated by androgens in rat Sertoli cells in vitro. *Reproduction* 2007; 133:1169–1179.

48. Beverdam A, Svingen T, Bagheri-Fam S, Bernard P, McClive P, Robson M, Khojasteh MB, Salehi M, Sinclair AH, Harley VR, Koopman P. Sox9-dependent expression of *Gstm6* in Sertoli cells during testis development in mice. *Reproduction* 2009; 137:481–486.
49. Mukherjee SB, Aravinda S, Gopalakrishnan B, Nagpal S, Salunke DM, Shaha C. Secretion of glutathione S-transferase isoforms in the seminiferous tubular fluid, tissue distribution and sex steroid binding by rat *GSTM1*. *Biochem J* 1999; 340(pt 1):309–320.
50. Fulcher KD, Welch JE, Klapper DG, O'Brien DA, Eddy EM. Identification of a unique mu-class glutathione S-transferase in mouse spermatogenic cells. *Mol Reprod Dev* 1995; 42:415–424.
51. Hewitt KJ, Agarwal R, Morin PJ. The claudin gene family: expression in normal and neoplastic tissues. *BMC Cancer* 2006; 6:186.
52. Oliveira SS, Morgado-Diaz JA. Claudins: multifunctional players in epithelial tight junctions and their role in cancer. *Cell Mol Life Sci* 2007; 64:17–28.
53. Swisshelm K, Macek R, Kubbies M. Role of claudins in tumorigenesis. *Adv Drug Deliv Rev* 2005; 57:919–928.
54. Benbrahim-Tallaa L, Siddeck B, Bozec A, Tronchon V, Florin A, Friry C, Tabone E, Mauduit C, Benahmed M. Alterations of Sertoli cell activity in the long-term testicular germ cell death process induced by fetal androgen disruption. *J Endocrinol* 2008; 196:21–31.
55. Bauche F, Fouchard MH, Jegou B. Antioxidant system in rat testicular cells. *FEBS Lett* 1994; 349:392–396.
56. Beckman JK, Coniglio JG. A comparative study of the lipid composition of isolated rat Sertoli and germinal cells. *Lipids* 1979; 14:262–267.
57. Franco R, Sanchez-Olea R, Reyes-Reyes EM, Panayiotidis MI. Environmental toxicity, oxidative stress and apoptosis: manage a trois. *Mutat Res* 2009; 674:3–22.
58. Byers S, Graham R, Dai HN, Hoxter B. Development of Sertoli cell junctional specializations and the distribution of the tight-junction-associated protein ZO-1 in the mouse testis. *Am J Anat* 1991; 191:35–47.
59. Ahmed EA, Barten-van Rijbroek AD, Kal HB, Sadri-Ardekani H, Mizrak SC, van Pelt AM, de Rooij DG. Proliferative activity in vitro and DNA repair indicate that adult mouse and human Sertoli cells are not terminally differentiated, quiescent cells. *Biol Reprod* 2009; 80:1084–1091.
60. Gilleron J, Carette D, Durand P, Pointis G, Segretain D. Connexin 43 a potential regulator of cell proliferation and apoptosis within the seminiferous epithelium. *Int J Biochem Cell Biol* 2009; 41:1381–1390.
61. Iida H, Noda M, Kaneko T, Doiguchi M, Mori T. Identification of rab12 as a vesicle-associated small GTPase highly expressed in Sertoli cells of rat testis. *Mol Reprod Dev* 2005; 71:178–185.
62. Session DR, Fautsch MP, Avula R, Jones WR, Nehra A, Wieben ED. Cyclin-dependent kinase 5 is expressed in both Sertoli cells and metaphase spermatocytes. *Fertil Steril* 2001; 75:669–673.
63. Chapman DL, Wolgemuth DJ. Isolation of the murine cyclin B2 cDNA and characterization of the lineage and temporal specificity of expression of the B1 and B2 cyclins during oogenesis, spermatogenesis and early embryogenesis. *Development* 1993; 118:229–240.
64. Liu D, Matzuk MM, Sung WK, Guo Q, Wang P, Wolgemuth DJ. Cyclin A1 is required for meiosis in the male mouse. *Nat Genet* 1998; 20:377–380.
65. Sharpe RM, McKinnell C, Kivlin C, Fisher JS. Proliferation and functional maturation of Sertoli cells, and their relevance to disorders of testis function in adulthood. *Reproduction* 2003; 125:769–784.
66. Britt DE, Yang DF, Yang DQ, Flanagan D, Callanan H, Lim YP, Lin SH, Hixson DC. Identification of a novel protein, LYRIC, localized to tight junctions of polarized epithelial cells. *Exp Cell Res* 2004; 300:134–148.
67. Young RH. Sex cord-stromal tumors of the ovary and testis: their similarities and differences with consideration of selected problems. *Mod Pathol* 2005; 18(suppl 2):S81–S98.
68. Young RH. Testicular tumors—some new and a few perennial problems. *Arch Pathol Lab Med* 2008; 132:548–564.
69. Meng J, Holdcraft RW, Shima JE, Griswold MD, Braun RE. Androgens regulate the permeability of the blood-testis barrier. *Proc Natl Acad Sci U S A* 2005; 102:16696–16700.
70. Fritz IB, Burdzy K, Setchell B, Blaschuk O. Ram rete testis fluid contains a protein (clusterin) which influences cell-cell interactions in vitro. *Biol Reprod* 1983; 28:1173–1188.
71. Magre S, Jost A. The initial phases of testicular organogenesis in the rat. An electron microscopy study. *Arch Anat Microsc Morphol Exp* 1980; 69:297–318.
72. Guillemot L, Citi S. Cingulin regulates claudin-2 expression and cell proliferation through the small GTPase RhoA. *Mol Biol Cell* 2006; 17:3569–3577.
73. Matter K, Aijaz S, Tsapara A, Balda MS. Mammalian tight junctions in the regulation of epithelial differentiation and proliferation. *Curr Opin Cell Biol* 2005; 17:453–458.